ELECTRICAL ENGINEERING
UNIVERSITY of WASHINGTON

# HVAC OPERATION IN A MULTI-STEP AHEAD TRANSACTIVE FRAMEWORK

Deliverables UW6 and UW7 of the project: "Transactive Campus Energy Systems: An R&D Testbed for Renewables Integration, Energy and Grid Services"

Rémy Rigo-Mariani
Tu. A. Nguyen
Miguel Ortega-Vazquez
Daniel Kirschen

***August 2016***

# Table of Contents:

# ABSTRACT

It has been extensively shown that smart controls of building loads, especially the Heating, Ventilation and Air-Conditioning (HVAC), can enhance power systems' management, facilitate energy savings and increase the hosting capacity for renewable energy sources. In addition to conventional demand response programs, a new paradigm called "transactive control" has emerged. This paradigm relies on market mechanisms in a multi-agent framework. This report describes the implementation of this framework using a bi-level optimization of the operation of the HVAC of an existing building. On the end-user side a multi-step optimal control performs arbitrage among cost, comfort and the ability to respond to transactive signals. On the utility side an outer optimization loop is introduced to find the most appropriate price signal to send to the building in order to encourage it to follow a predefined power profile. An artificial neural network (ANN) is used to implement the Model Predictive Control (MPC) while a finer model in EnergyPlus simulates the building control and allows computing the prediction error. Simulations are performed with different settings of the building. Finally, a case with several buildings is investigated.

# ACKNOWLEDGMENTS

The work presented in this report was carried out as part of the Clean Energy and Transactive Campus project in partnership with the Pacific Northwest National Laboratory (PNNL) and Washington State University (WSU). This project was supported by both the U.S. Department of Energy and the Washington State Department of Commerce Clean Energy Fund. The authors would like to thank PNNL for providing the Energy Plus model of the building and their valuable advice on how to implement the co-simulation environment.

# ACRONYMS

| | | |
|---|---|---|
| ANN | : | Artificial Neural Network |
| ASHRAE | : | American Society of Heating Refrigerating and Air Conditioning Engineers |
| DR | : | Demand Response |
| E+ | | Energy Plus / Energy+ |
| GAMS | : | General Algebraic Modeling System |
| GD | : | Greedy Method |
| HVAC | : | Heating, Ventilation and Air-Conditioning |
| MILP | : | Mixt Integer Linear Programming |
| MLP | : | Multi-Layer Perceptron |
| MPC | : | Model Predictive Control |
| PMV | : | Predictive Mean Vote |
| PSO | : | Particle Swarm Optimization |
| RMSE | : | Root Mean Square Error |
| SEB | : | Science Engineering Building |
| TCL | : | Thermostatically Controlled Load |
| TE | : | Transactive Energy |
| TMY | : | Typical Meteorological Year |
| TS | : | Transactive Signal |

# LIST OF SYMBOLS

| | | | |
|---|---|---|---|
| $T^z$ | : | Zone temperature | $^oC$ |
| $T^z_{set}$ | : | Zone temperature set point | $^oC$ |
| $T_{out}$ | : | Outdoor temperature | $^oC$ |
| $T_{ref}$ | : | Comfort temperature | $^oC$ |
| $P_{hvac}$ | : | HVAC power | kW |
| $U$ | : | Building Utility Function | - |
| $\alpha_C$ | : | Coefficient attached to the cost minimization | - |
| $\alpha_T$ | : | Coefficient attached to the comfort maximization | - |
| $\alpha_E$ | : | Coefficient attached to the flexibility maximization | - |
| $\tau$ | : | Price-like transactive signal | p.u. |
| $N_z$ | : | Number of zones | - |
| $F_a$ | : | Neuron activation function | - |
| $T_{start}$ | : | Starting time step for the MPC optimization | h |
| $T_{end}$ | : | Ending time step for the MPC optimization | h |
| $T_{step}$ | : | Prediction horizon (in number of steps) | - |
| $N_i$ | : | Number of input neurons | - |
| $N_h$ | : | Number of hidden neurons | - |
| $N_o$ | : | Number of output neurons | - |
| $P_{target}$ | : | Power to follow for the aggregating entity | kW |
| $P_{target\_corr}$ | : | Corrected power to follow for the aggregating entity | kW |
| $P_{hvac\_meas}$ | : | Simulated measured HVAC power | kW |
| $R_{th}$ | : | Thermal resistance | $^oC/kW$ |
| $C_{th}$ | : | Thermal capacitance | $kWh/^oC$ |
| $COP$ | : | Coefficient of performance | - |
| $T_{out\_max}$ | : | Design outdoor temperature | $^oC$ |
| $T_{set\_min}$ | : | Minimum design set point | $^oC$ |

# 1 INTRODUCTION

## 1.1 Motivation and Architecture Overview

According to the latest survey conducted by the U.S. Energy Information Administration, residential and commercial buildings account for 40 % of the global energy consumption [EIA 16]. In commercial buildings the Heating, Ventilation and Air-Conditioning (HVAC) systems represent about 45% of the energy consumed. Optimal management of HVAC in building is thus perceived as a significant opportunity for reducing energy use and to enhance the efficiency of the power system as a whole. As reviewed in [Kok 16], many approaches are investigated to control buildings from the utility side. While conventional Demand Response (DR) programs (Fig.1*a*) have proven somewhat effective, one of the main drawback is that the full response of the devices is not available because their actual state is not known. Two-way communications approaches allow more flexible controls and smarter operations (Fig.1*b*). However, these methods quickly reach the limits of computational capabilities because their complexity increases with the number of actors. Furthermore, such centralized approaches are limited by privacy issues if a supplier needs to model the behavior and preferences of the building users.

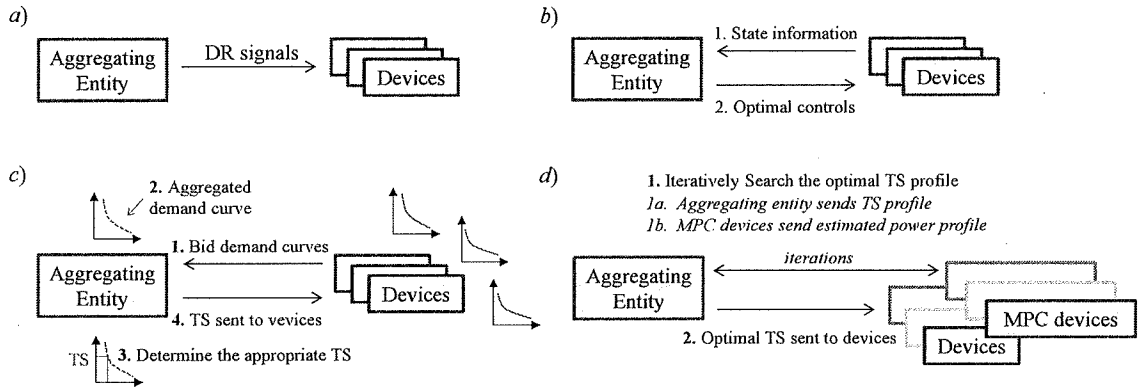


Fig.1: Building control architecture - *a)* Demand Response - *b)* Central Optimization – *c)* Bid-auction market – *d)* Chosen architecture for multi-step ahead transactions

Transactive Energy (TE) provides a framework where supply and demand actors interact using a bid-auction mechanism with a price-like signal called Transactive Signal (TS). The end users submit their bids in the form of demand curves that map their expected consumption to the TS. The aggregating entity then matches the overall demand curve with a supply curve or a supply objective and constraints. The resulting TS is then sent back to the devices that act according to the received value (Fig.1*c*). The first proof of concept was the Olympic Peninsula Demonstration project [Hammerstrom 07] with the control of the space heating of 112 houses using gateways that supported two-ways communication. Since then many investigations have been performed to study the possibility to provide specific ancillary services such as frequency regulation or spinning reserve [Subbarao 13]. One of the main advantages of this multi-agent approach is its scalability. Since the proposed framework considers different actors/users distributed in the grid, then it can also be applied to describe the interaction between the equipment within a given system. For instance [Hao 16] designs a double auction market within a building to optimally control the HVAC loads considering the electricity, water and gas markets.

In the transactive framework, the market clears at every time step and the corresponding controls are sent to the devices using an appropriate TS. This report investigates a new, multi-step transactive approach. Rather than performing an optimal multi-hour scheduling, the objective is to improve the sub

hourly decision making by estimating the state of the system over a longer period of time. For instance a given amount of energy at time $t$ will correspond to a higher price if it could lead at a critical situation for the next time steps. In that multi step ahead framework, time-dependent TS are generated by considering the system behavior over a receding horizon (15 min in the simulation with a time step of 5 min). Because the demand curves are not formulated explicitly, an iterative search method is used on the aggregating entity side to find the optimal TS profile that have to be sent to the devices (Fig.1*d*).

This multi-step transactive approach is combined with a Model Predictive Control (MPC) on the building side and the approach is tested on the HVAC system of the System Engineering Building (SEB) on the Pacific Northwest National Laboratory (PNNL) campus in Richland, WA. The behavior of the SEB is simulated using a model of this building developed using the Energy Plus tool. As in [Ma 11], the zone temperature set points $T^z_{set}$ depending and the objective to follow (cost minimization, comfort, etc) are computed using MATLAB®. The controls are sent to EnergyPlus which then returns buildings information for the corresponding time step including the building HVAC consumption $P_{hvac}$ and the zone temperatures $T^z$ (Fig.2). The outdoor temperature $T_{out}$ is also an output of Energy Plus which performs the simulations based on TMY data. A co-simulation MATLAB/Energy+ tool [Bernal 12] [Zhao 13] provides the environment for these simulations.

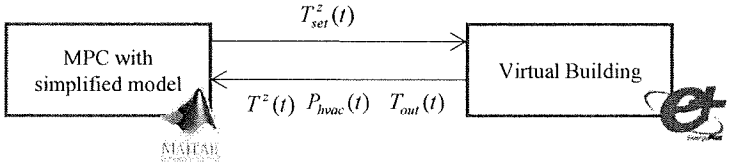


Fig.2: Co-simulation Matlab/Energy Plus

## 1.2 Organization of the report

- Section 2 describes the model of the Systems Engineering Building (SEB) using Artificial Neural Networks (ANNs) to predict the energy consumption based on the outdoor temperature and the controlled set points.

- Section 3 presents in detail the MPC strategy which achieves a trade-off between energy savings and comfort. An additional component is introduced in the utility function to incorporate the building's willingness to respond to incentives.

- Section 4 describes the implementation of the transactive framework using a bi-level optimization that optimizes the TS profile in order to follow a predefined profile on the supplier side. Different building preferences are investigated.

- Section 5 considers the management of multiple buildings.

# 2 SYSTEMS ENGINEERING BUILDING MODEL

## 2.1 Buildings Modeling

### 2.1.1 Modeling approaches

The first step of the presented work consisted in choosing an appropriate simplified model for the building under study. A compromise is found between complexity and computation time before integrating this model in the MPC strategy. Similarly to other areas of study such as weather forecasting for renewable production, models used to predict a building's energy consumption, and can be divided into two main classes: physical models and statistical models [Foucquier 13]. Multi-zone nodal methods, such as the algorithms embedded in EnergyPlus or TrnSys, are the simplest physical models. Good accuracy can be obtained with an extensive description of the system (solar radiation, materials, HVAC configuration, occupancy, *etc.*). However they do not provide an explicit model [Privara 13] and the computation time makes them unfit for any MPC approach that would require several runs of the model in order to find the optimal controls.

Statistical methods such as machine learning or Autoregressive Moving Average (ARMA) provide simple representations of the system that can be integrated easily in an optimization process. Those approaches do no required any physical information on the system under study and are based on the implementation of a function deduced solely from samples of training data. This document therefore describes an Artificial Neural Network (ANN) to predict the HVAC consumption. Two distinct ways of using the ANNs for energy consumption can be identified. First they can be implemented purely for forecasting purposes based on meteorological data and occupancy [Plaudel 14]. For instance [Gossard 13] or [Magnier 10] use ANN forecast as a simple and fast model to optimize the building structure considering energy saving and comfort criteria. The second way of considering the ANN for building HVAC consumption is closer to the scope of this study. It consists in actually exploiting the models to predict the energy consumption depending on the control strategy. Such models are then used to show how a smart management of the building with optimal set points minimizes the energy cost while fulfilling comfort constraints as in [Kusiak 14] and [Lee 15].

### 2.1.2 Multi-Layer Perceptron (MLP)

One widely used ANN structure for prediction is the feed forward multi-layer perceptron (MLP) [Raza 15] whose architecture is shown on Fig.3*a* with 2 inputs neurons; one output neuron and a hidden layer with 3 neurons. The term feed forward refers to the unidirectional flow of information from the input to the output through the hidden layers.

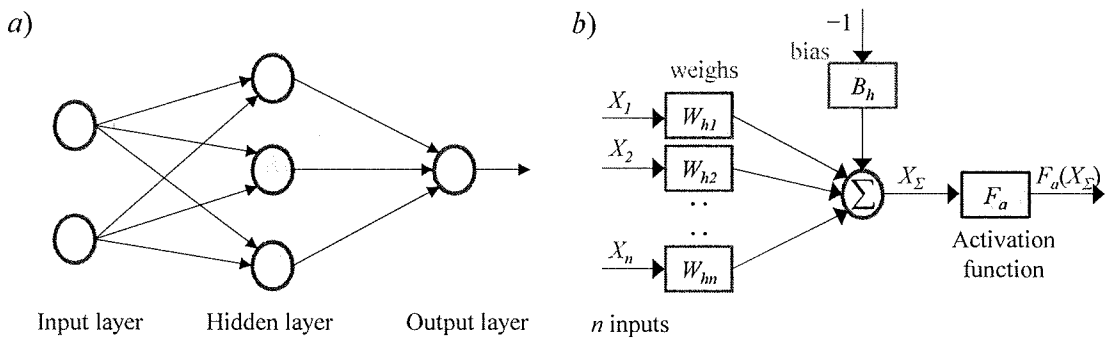


Fig.3: Multi-Layer Perceptron – a) ANN architecture – b) Neuron architecture

Fig.3*b* shows the basic function of the neurons that performs a linear weighted combination of the inputs with a bias. This sum is then passed thought an activation function $F_a$. Typically for forecasting purposes that function is a sigmoid (Fig.4*a*) or hyperbolic tangent (Fig.4*b*). In this work the ANN used to represent the building is to be modeled in GAMS to perform an optimization based on mixed integer linear programming (MILP). Therefore, as in [Lee 15], a bipolar linear activation function is used to simplify the implementation (Fig.4*c*). Here the number of inputs neurons is equal to the number of inputs for the forecast models and those neurons are not subject to any activation function. The output neurons that correspond to the prediction are implemented using a linear activation function.

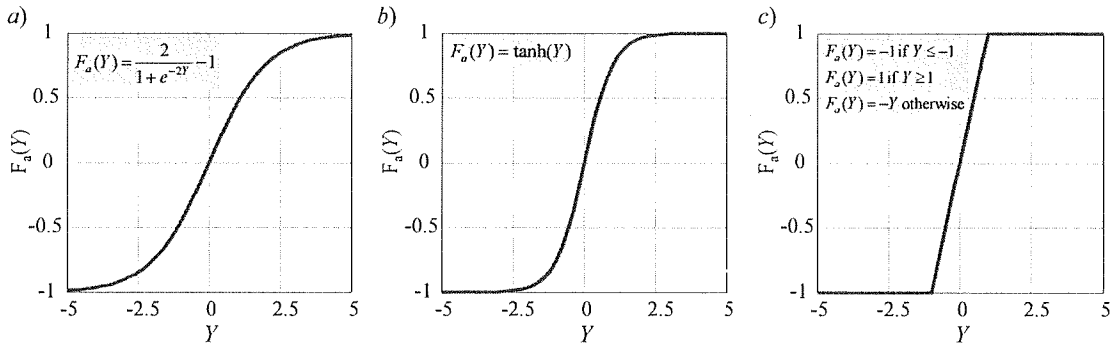


Fig.4: Activation Function - a) Sigmoid - b) hyperbolic tangent - c) bipolar linear

Four main steps are required to implement a neural network for prediction:

### 1. Determine the inputs

The first step is to select the appropriate set of input variables. For energy consumption forecast in building many different sets of variables can be used: meteorological parameters [Macas 16] (solar radiation, cloud covering, wind speed/direction etc.), HVAC operation details [Kusiak 14] (temperature/pressure set points, chilled water temperature, valve positions, etc.). The order of the autoregressive model can also be an adjustable input variable. In the present study the only exogenous variable considered is the outdoor temperature.

### 2. Determine the ANN architecture

The architecture of the MLP has then to be chosen in terms of the number of hidden layers and the number of neurons in each layer (in most cases a single hidden layer is sufficient). Just like the set of

input variables, the MLP structure can be determined using an optimization or selection process [Macas 16] and can have a strong influence on the accuracy of the prediction.

**3. Train the ANN**

The ANN training consists in finding the neurons weight and bias using back propagation methods that minimize the RMSE or the absolute error by computing the Jacobian of the model error. The most widely used method is the Levenberg–Marquardt Training [Yu 11] and its implementation in the MATLAB Neural Network Toolbox is considered in the study. Note that the training dataset has a strong influence on the final accuracy of the estimator.

**4. Test the ANN**

Once the network is trained an additional set of data is used to estimate the performance of the generated model.

### 2.1.3 Multi-steps ahead prediction

The objective of the study is to develop a MPC based on a multi-step prediction. When considering multi-period forecasts three different approaches can be adopted for the model architecture [Boné 02]. The first commonly used method consist in performing the estimation for the next time step and feedback the results in the inputs of a regressive model until the desired prediction horizon is reached (Fig.5*a*). This method is the simplest one but the accumulated error can lead to a strong divergence for long horizons.

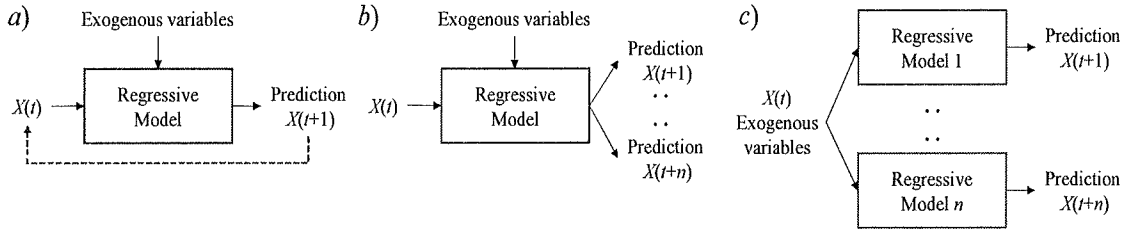


Fig.5: Multi-steps ahead forecast – *a*) iterative – *b*) multi step model – *c*) multi models

Another alternative is based on a global approach to forecast all the time steps in the prediction horizon at once (Fig.5*b*). In this case no guarantee is given that a model can fit properly the entire horizon and some accuracy can even be lost for the first steps. The third option consists in one prediction model per step (Fig.5*c*). This requires a more complex implementation and training. The present work only considers the first simple iterative approach.

## 2.2 SEB Model

### 2.2.1 Objective

The objective of this study is to develop a MPC strategy to control the Systems Engineering Building on the PNNL campus in Richland, WA. The starting point of the work is an Energy Plus model of this building with the following characteristics:

- 33 temperature zones identified

- 17 zones controlled using the temperature set points ($N_z = 17$)
- Building in cooling mode only (summer week considered)
- Simulations performed with a time step of 5 min

### 2.2.2 Model architecture

Some works in the literature give examples of multi-outputs neural networks that forecast both temperature and humidity [Zaheer 04] or comfort index and consumption [Yuce 14]. In the present work the choice is made to dissociate the temperature and the HVAC consumption models as well as the outdoor temperature prediction [Macas 16] (Fig.6). Furthermore, the meteorological variables are limited to the outdoor temperature only and every zone is modeled independently to predict the corresponding temperature $T^z$. The only HVAC variables considered are the temperature set points for the seventeen controllable zones. Those set points are then control variables in the MPC simulation. As mentioned in the previous section, the outputs of the different models were iteratively used as inputs to perform the multi-step prediction.

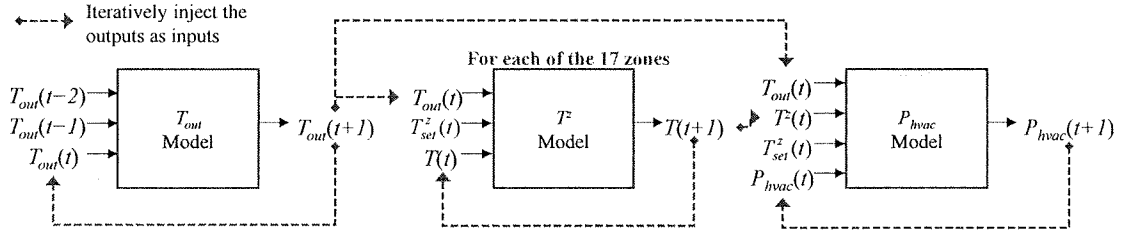


Fig.6: Model architecture for multi-steps ahead prediction

### 2.2.3 Training and Test Data sets

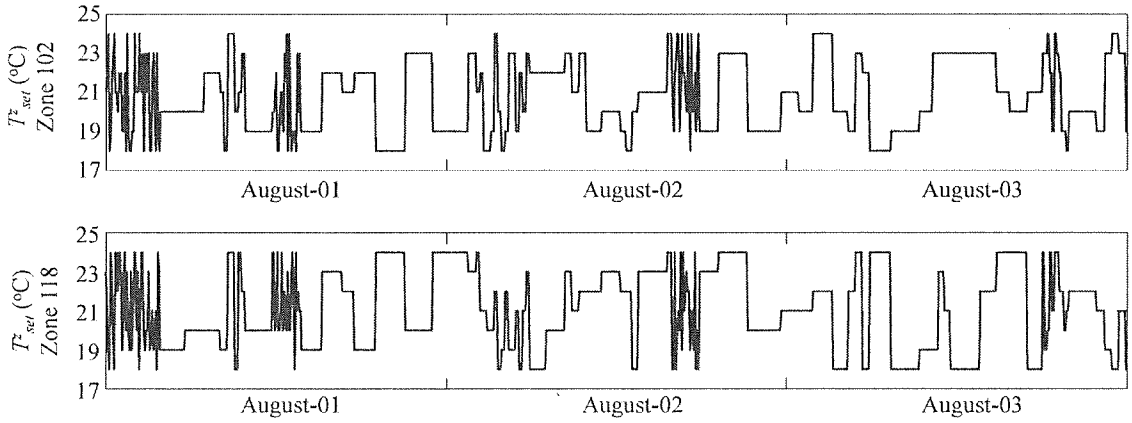


Fig.7: Samples of set points profile used to generate the training data set

The Energy Plus model is used to generate sets of training data to fit the coefficients of the temperatures and HVAC consumption models. Since the objective is to develop a model that takes into account various set points, the training data is produced by randomly changing the zone controls as shown on Fig.7. The set points for each zone were independently selected using a uniform probability distribution of the integers between 18 °C and 24 °C. The length of the period with constant set points was also subject to a random distribution with durations from 1 time step to 24 time steps (*i.e.*

respectively 5 min and 2h). The co-simulation is run and set points, zones temperatures as well as the HVAC consumption profiles are saved to be used as training data sets for the models. The test data set are generated the same way but with continuous values for the temperature set points. Note that in the simulation the HVAC is assumed to be on all day.

- Training data set: 5 simulations from August 01st to August 19th - 27360 points
- Testing data set: 1 simulation from August 20th to August 20th – 1728 points

### 2.2.4 Outdoor temperature

Since the MPC strategy is tested using the Energy Plus as a virtual representation of the building, the choice is made to use the TMY data embedded in Energy+ to generate the outdoor temperature forecast. A MLP with a single hidden layer with two hidden neurons is trained to minimize the RMSE error with the input structure illustrated in Fig.6. The preliminary results show a really low value of the RMSE for one step ahead prediction (*i.e.* 5 min) (Fig.8) with a relative error of 0.08 %. This high accuracy can be explained by the similarity between the outdoor temperatures of the training and testing data sets, which both relate to the month of August and have smooth profiles.

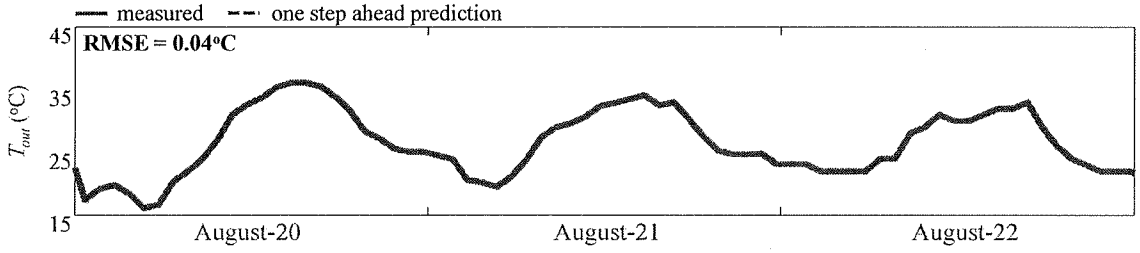


Fig.8: One step ahead prediction and measured outdoor temperature

Naturally the forecast error increases with the prediction horizon but the observed value remain very low with a RMSE of only 1 °C computed after five hundreds of random test samples (Fig.9*a*). Fig.9*b* shows a one hour ahead prediction which illustrates the small deviation between the predictions and the measured values.

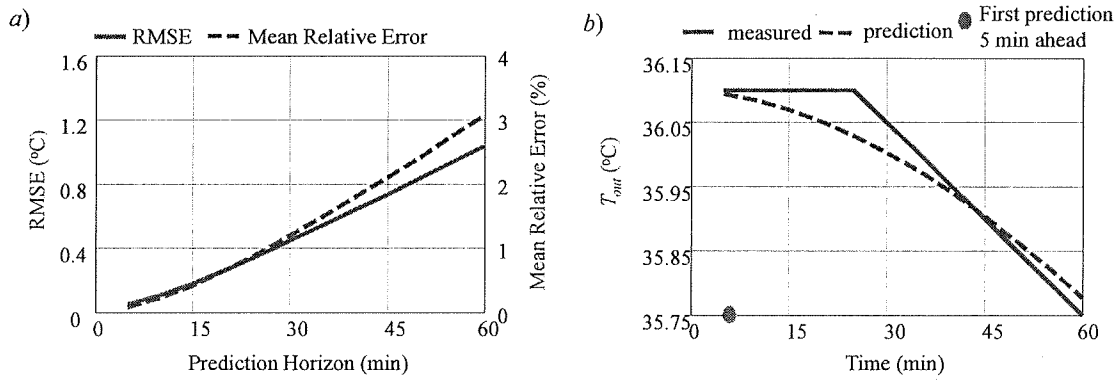


Fig.9: Multi-Step prediction for $T_{out}$ - *a)* forecast error - *b)* sample of 1 h ahead prediction

### 2.2.5 Zone temperature

Each zone temperature is modeled using the linear regression model given in Eq.1. The idea is to consider the difference $T^z(t) - T^z_{set}(t)$ as representative of the cooling energy and $T^z(t) - T_{out}(t)$ homogenous to the thermal losses with coefficients $a$ and $b$ between −1 and 0 into take account of the zone inertia.

$$C\frac{dT}{dt} = W_{HVAC} + W_{loss} \Rightarrow T^z(t+1) = T^z(t) + a \times \left(T^z(t) - T^z_{set}(t)\right) + b \times \left(T^z(t) - T_{out}(t)\right) \quad \textbf{Eq.1}$$

As mentioned above, the models are designed for multi step ahead prediction. Therefore, instead of fitting the coefficients to minimize the prediction error for the next period, longer profiles are considered to minimize the error over the entire prediction horizon. Such approach avoids focusing on regression models similar to persistent approaches that put a large weight on the coefficients attached to the temperature at time $t$ to predict the temperature at time $t + 1$. A hundred samples of six time steps (*i.e.* 30 min) were taken from the global training data for every zone. For each sample the training values for the set points and outdoor temperatures are used to compute the 6 steps ahead prediction $T^{pred}_{sample}$. Finally the fitting procedure aimed at minimizing the multi-period root mean square error $RMSE_{multi}$, with the training profile $T^{train}_{sample}$ as computed as in Eq.2. for each zone.

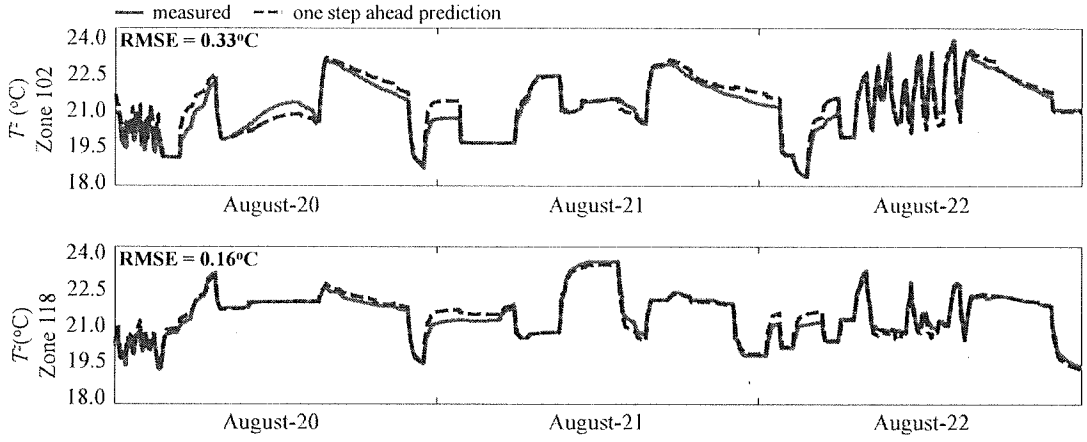


Fig.10: One step ahead prediction and measured zone temperature

$$RMSE_{multi} = \sqrt{\frac{1}{100 \times 6} \times \sum_{sample=1}^{100} \sum_{t=1}^{6} \left(T^{pred}_{sample}(t) - T^{train}_{sample}(t)\right)^2} \quad \textbf{Eq.2}$$

Fig.10 shows the results obtained for two zones for a one step ahead forecast with the corresponding error for the whole test set (i.e. 5 days). The overall RMSE considering the seventeen zones equals to 0.31 °C with a mean relative error of 0.92 %. As expected, the error increases when the forecast are performed for longer horizon of time with a good accuracy for one hour ahead predictions (Fig.11).

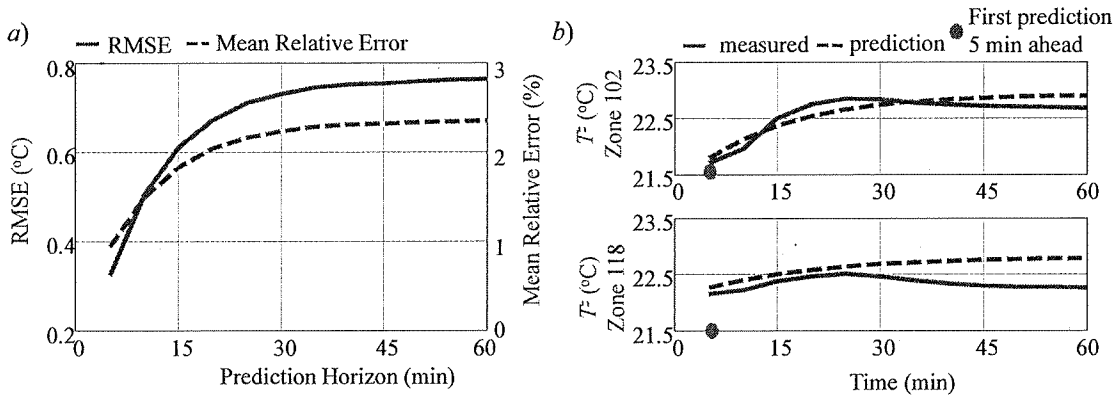


Fig.11: Multi-Step prediction for $T^{\circ}$ - a) forecast error - b) sample of 1 h ahead prediction

### 2.2.6 HVAC consumption

The last step of the modeling directly refers to the prediction of the HVAC consumption. Note that the multi-step forecast requires the output of the models described in the previous subsections for the outdoor and zone temperatures. With the architecture illustrated in Fig.6 the ANN used to predict the HVAC consumption has 36 inputs:

- 17 instantaneous zone temperatures
- 17 instantaneous zones temperature set points
- Instantaneous outdoor temperature
- HVAC consumption observed at the previous time step

Preliminary work requires training the $P_{hvac}$ neural network with one hidden layer and different numbers of hidden neurons. Just like for the outdoor temperature, the Neural Network MATLAB Toolbox is used to train the model using the Levenberg–Marquardt algorithm with random starting points [Hagan 94]. The objective is to find the most appropriate architecture that minimizes the error for one step ahead prediction. The results show that the number on hidden neurons does not have a significant impact on performance. Contrary to what could be expected, increasing the number of neurons does not necessarily improve the prediction. The observed error is actually greater for the largest number of neurons considered (Fig.12*a*). ). For the multi step forecast, the error is naturally greater for longer time horizons. Increasing the number of neurons slightly improves the prediction for a 15 min ahead prediction but the effect of any change in the number of neurons seems to have a random effect for 30 min and 1 h ahead (Fig.12*b*).

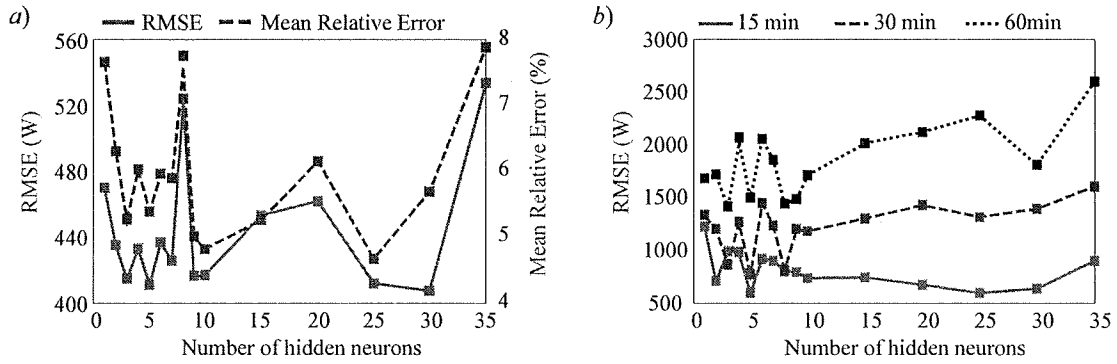


Fig.12: Impact of the number of hidden neurons - a) 5 min ahead - b) multi steps ahead

Another concern while investigating the neural network used to model the HVAC consumption is to check that it respects the physical behavior of the system because statistical approaches do not guarantee that this is the case. In the present study, after the training phase the resulting ANN is tested to control that the power correctly evolves with the zone temperature controls. A baseline test day corresponding to a constant set points of 21 $^{O}$C is recorded using the MATLAB/Energy+ co-simulation. Then at 1200 h the zone set points were progressively increased (or decreased) degree by degree ( $\Delta T^{z}_{ref}$ ) and the $P_{hvac}$ decrement (or increase) was analyzed to generate $\Delta P^{ref}_{hvac}$ for each zone. One thousand different neural networks with random numbers of hidden neurons (between 1 and 5) and random starting points are trained. The best architecture is chosen according to Eq.3 after testing the model for the baseline test day at 1200 h and generating the estimated $\Delta P_{hvac}$

$$\text{obj}: \min \sqrt{\frac{1}{N_z}\sum_{z=1}^{N_z}\left(\Delta P_{hvac}(\Delta T^{z}_{set}) - \Delta P^{ref}_{hvac}(\Delta T^{z}_{set})\right)^2} \quad \text{s.t}: \frac{\Delta P_{hvac}}{\Delta T_{set}} \le 0 \ \ \forall\, zone \qquad \textbf{Eq.3}$$

Based on these results, a neural network with 5 hidden neurons is chosen. Fig.13 shows the $\Delta P_{hvac}$ for every zone compared to the reference values. While the physical behavior of the model complies with the constraints $\Delta P_{hvac} / \Delta T_{set} \le 0$, the behavior of some zones is not accurate for $\Delta T_{set} = -3$ $^{O}$C (Fig.13*a*). In particular, the effect of a change in the set-point for zone 14 is underestimated while it is overestimated for zone 9. On the other hand, the results are more accurate for $\Delta T_{set} = +3$ $^{O}$C. In this case, $\Delta P_{hvac}$ follows the reference more closely for most zones (Fig.13*b*). Even if some errors appear significant, the baseline power is 9.7 kW with a computed mean relative error of 7.6 % for the $P_{hvac}$ prediction.

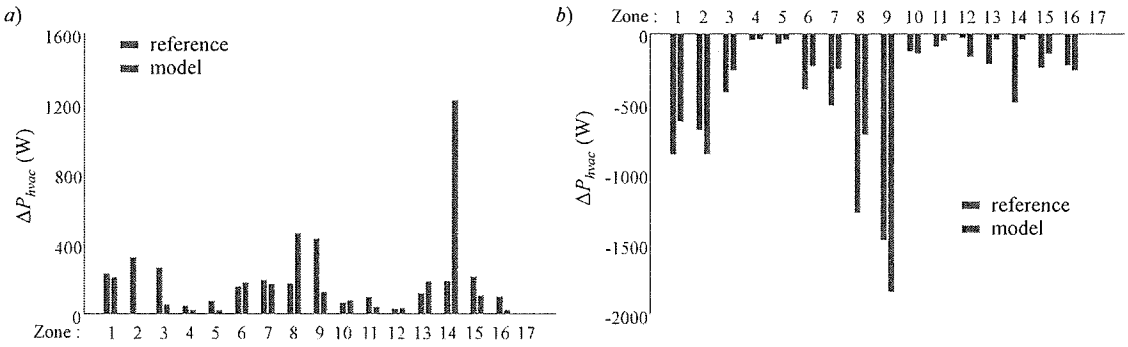


Fig.13: Performance of the selected model regarding $\Delta P_{hvac}$ – *a)* $\Delta T_{set} = -3$ $^{O}$C – *b)* $\Delta T_{set} = +3$ $^{O}$C

Fig.14 shows the model behavior for the same baseline day but with different values of $\Delta T_{set}$. It can be observed that the $P_{hvac}$ variations are greater for larger changes in the temperature set points. Also the model globally respects the ranking of the most and least influential zones with positive and negative $\Delta T_{set}$. For instance, zone 9 has the largest effect on the HVAC consumption while zones 1, 2 and 3 or 13, 14 and 15 have an average effect. Changing the control for zone 17 has no observable impact on $P_{hvac}$. Indeed the restrooms associated with that zone are not controllable in the Energy Plus model [Hao 16].

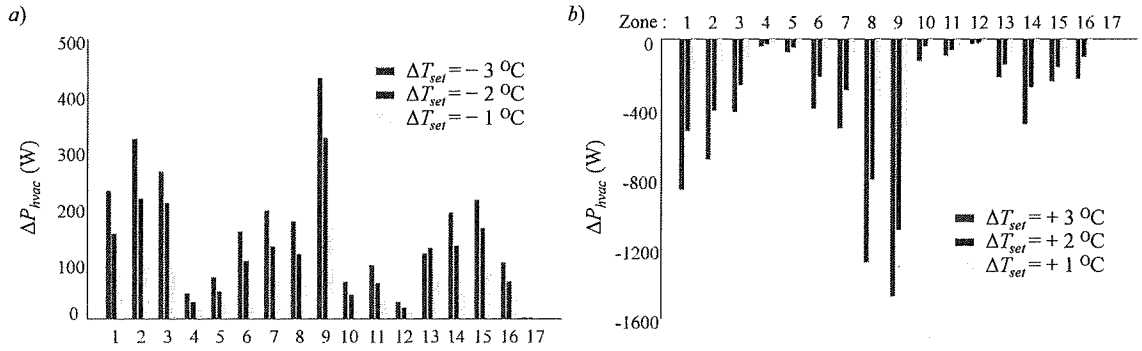


Fig.14: $\Delta P_{hvac}$ for the selected model– *a)* $\Delta T_{set}$ < °C – *b)* $\Delta T_{set}$ > 0 °C

Fig.15 shows the error for the one step ahead prediction for a couple of days with a RMSE of 505 W and a mean relative error of 5.6 % while considering the full testing set of five days. Five hundred random test samples were used to compute the error for the multistep forecast. Fig.16 shows that, as expected, the error increases for longer time horizons.

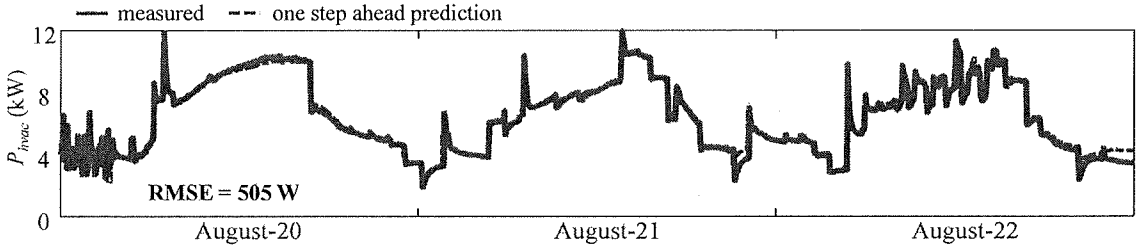


Fig.15: One step ahead prediction and measured HVAC consumption

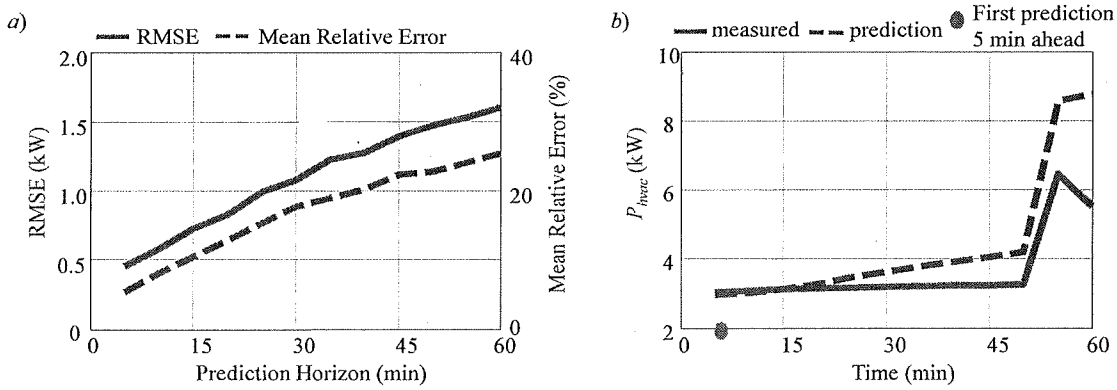


Fig.16: Multi-Step prediction for $P_{hvac}$ - a) forecast error - b) sample of 1 h ahead prediction

The forecast error increases with the prediction horizon and thus has a direct impact on the performance of the multi-step ahead MPC control. Thus with the observed values (more than 20 % relative error for 1 h ahead) it does not make sense to use such a model for a multi-hour scheduling with a time step of 5 min. Even for sub-hourly prediction the prediction error can be significant. Aggregating multiple buildings could reduce the error. This is investigated in the last section of this document.

# 3 MODEL PREDICTIVE CONTROL

## 3.1 Utility Function

At the building level, the model developed in the previous section is used to implement a MPC strategy. As described before, the goal is to perform a multi-step optimization (from $T_{start}$ to $T_{end}$) of the set points to minimize an explicit utility function. One of the first objectives is to minimize the cost while fulfilling comfort constraints. This is not a new approach and there are many examples of such objective functions in the literature. If the expression of the cost noted $U_C$ is straightforward with a price profile $\tau$ (Eq.4) different ways of computing the comfort can be used. The simplest method to ensure comfort consists in assigning bounds for the zone temperature as in [Kusiak 14] or [Ma 11]. Other approaches refer to the Predictive Mean Vote (PMV), an index originally developed in [Fanger 72] that has been used to create the ASHRAE standards (American Society of Heating Refrigerating and Air Conditioning Engineers). A comfort scale [− 3, 3] is defined considering metabolic rate, clothing insulation, air temperature and humidity, air velocity, and the mean radiant temperature. [Fereira 12] develops a ANN model to predict the PMV. The energy consumption is then minimized while ensuring that the index remains within specified bounds. In this study the comfort constraint is directly included in the objective function (noted $U_T$) as in [Lee 15] and is expressed as a deviation of the zone temperature from a reference value $T_{ref}$ (arbitrary set at 21 $^{O}$C for all zones) (Eq.5).

$$U_C = \sum_{t=T_{start}}^{T_{end}} P_{hvac}(t) \times \tau(t) \qquad \textbf{Eq.4}$$

$$U_T = \sum_{t=T_{start}}^{T_{end}} \sum_{z=1}^{N_z} \left| T^z(t) - T_{ref} \right| \qquad \textbf{Eq.5}$$

One of the objectives of the proposed control is the ability to respond to incentives. Considering only comfort or cost could lead to a reduction of the range for the HVAC power. Thus a contribution of this study is to include an additional component in the utility function to represent price elasticity. As expressed in Eq.6 the elasticity $e$ is a measure of the change in demand in response to a change in the price of electricity from reference values indexed with "0" [Patteeuw 15].

$$e = \frac{\tau^0}{P_{hvac}^0} \times \frac{\partial P_{hvac}}{\partial \tau} \Rightarrow e = \frac{\tau^0}{T_{set}^{z0}} \times \frac{\partial T_{set}^z}{\partial \tau} \qquad \textbf{Eq.6}$$

$$U_E = \sum_{t=T_{start}}^{T_{end}} \sum_{z=1}^{N_z} \left| \frac{\tau^{0N}}{T_{set}^{z0N}} \times \frac{\partial T_{set}^{zN}}{\partial \tau^N} - 1 \right| \qquad \textbf{Eq.7}$$

Depending on the meteorological conditions and the occupancy of the building the range of reachable values for the HVAC consumption can be reduced by moving the set points. Thus for some

particular points the elasticity could be equal to zero over a wide range, which means that changing the price would not have any significant effect on the energy consumption. To match the controllability of the HVAC with the price evolution, the elasticity expression is rewritten considering the set points (Eq.6) with the minimum (resp. maximum) set point corresponding to the minimum (resp. maximum) price in cooling mode. The idea is to implicitly enforce the bid curve of the building as proposed in [Schneider 11] and [Hammerstrom 07]. A term $U_E$ is then added to the utility function working with normalized values indexed "$N$") (Eq.7).

Finally, all these components are integrated in a single utility function $U$, which consists of a sum of the objectives, normalized using their expected maximum values. Weights $\alpha_C$, $\alpha_T$ and $\alpha_E$ are introduced to give priority to one or the other component (Eq.8). $T_{step}$ is the time horizon for the optimization in number of steps between $T_{start}$ and $T_{end}$ and the maximum expected temperature deviation from the reference is 3 °C (set points between 18 °C and 24 °C and $T_{ref}$ = 21 °C).

$$U = \alpha_C \times \frac{U_C}{P_{hvac}^{max} \times \sum_{t=T_{start}}^{T_{end}} \tau(t)} + \alpha_T \times \frac{U_T}{T_{step} \times N_z \times 3} + \alpha_E \times \frac{U_E}{T_{step} \times N_z} \qquad \textbf{Eq.8}$$

Based in the manner in which the utility function is expressed, the priority coefficients refer to the whole building and are shared by all the zones. However, the comfort and elasticity objectives could be "discretized" with preferences set for each individual zone. For instance, priority could be given to some zones to respond to incentives while other parts of the building would be unresponsive to the transactive signal and set to provide maximum comfort. That aspect has no be studied in the present work but could be part of further investigations.

## 3.2 GAMS Implementation

The MPC building controller is implemented in GAMS. The goal is to minimize the previously defined objective function by finding the optimal temperature set points over time for all the zones $\mathbf{T^{z^*}_{set}}$ (i.e. $N_z \times T_{step}$ decision variables) within specified bounds.

$$\mathbf{T^{z^*}_{set}} = \underset{\substack{18 \le T^z_{set} \le 24 \\ \forall t \in [1..T] \\ \forall z \in [1..N_z]}}{\arg\min}(U) \quad \text{s.t} \quad \text{model equations} \qquad \textbf{Eq.9}$$

Constraints are introduced in order to take the model equation into account. In particular, the implementation of the neural network require the introduction of a new set of continuous and binary variables. The following paragraph presents a generic way to implement a Neural Network in GAMS.

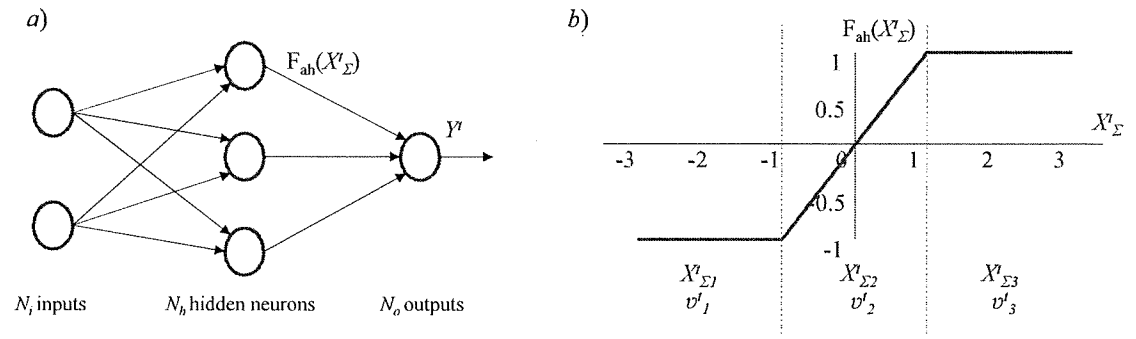


Fig.17: Feed-forward MLP - *a)* architecture - *b)* activation function for hidden neurons

Fig.17 evokes the architecture of a feed-forward Multi-Layer Perceptron with a bipolar linear activation function $F_{ah}$ for the hidden neurons. $N_i$, $N_h$ and $N_o$ are respectively the number of input, hidden and outputs neurons. For the outputs neurons a pure linear function is considered. At each time step of the prediction the instantaneous neural network inputs are stored in a vector $\mathbf{X^t}$. Then the first set of constraints ($N_h \times T_{step}$ constraints) referring to the model equations concern the linear combination of the inputs noted $X^t_\Sigma$ using the weights $\mathbf{W_h}$ and bias $B_h$ of each hidden neuron (Eq.10). As shown on Fig.17*b*, for every neurons and at every time step, three continuous variable ($X^t_{\Sigma 1}$, $X^t_{\Sigma 2}$, $X^t_{\Sigma 3}$) and three binary variables ($v^t_1$, $v^t_2$, $v^t_3$) are introduced to perform a piece wise linearization of the activation function. Then $8 \times N_h \times T_{step}$ constraints are written (Eq.11 to Eq.15) where $M$ is the expected maximum absolute value of $X^t_\Sigma$ (typically 10). The outputs of the hidden neurons are then stored in a vector $\mathbf{F^t_{ah}}$ and Eq.16 is used to compute the neural network outputs $Y^t$ for each time step ($N_o \times T_{step}$ constraints).

$$X^t_\Sigma = \mathbf{X^t}.\mathbf{W_h} + B_h \quad \textbf{Eq.10}$$

$$-M \times v^t_1 \le X^t_{\Sigma 1} \le -v^t_1 \quad \textbf{Eq.11}$$

$$-v^t_2 \le X^t_{\Sigma 2} \le v^t_2 \quad \textbf{Eq.12}$$

$$v^t_3 \le X^t_{\Sigma 3} \le M \times v^t_3 \quad \textbf{Eq.13}$$

$$X^t_\Sigma = X^t_{\Sigma 1} + X^t_{\Sigma 2} + X^t_{\Sigma 3} \quad \textbf{Eq.14}$$

$$F_{ah}\left(X^t_\Sigma\right) = X^t_{\Sigma 2} - v^t_2 + v^t_3 \quad \textbf{Eq.15}$$

$$Y^t = \mathbf{F^t_{ah}}.\mathbf{W_o} + B_o \quad \textbf{Eq.16}$$

Considering the constraints that affect the input values for every time step, the modeling of a standard MLP for multi steps ahead forecast requires:

- $(N_i + 5 \times N_h + N_o) \times T_{step}$ continuous variables
- $3 \times N_h \times T_{step}$ binary variables
- $(N_i + 9 \times N_h + N_o) \times T_{step}$ constraints

For instance, for a three steps ahead optimization of the temperature set points and with the chosen architecture for the $T_{out}$ and $P_{hvac}$ neural networks, the model implementation requires 228 continuous variables, 21 binary variables and 319 constraints. Note that the computation of the absolute values to

express the utility function also requires additional continuous variables (positive and negative components) and constraints that are not included in those numbers.

### 3.3 Sample Demand Curves

Before describing the integration of the MPC in a transactive framework, it is useful to examine how the expected demand curves for the building depend on the settings ($\alpha_C$, $\alpha_T$ and $\alpha_E$). In a transactive market a demand curve corresponds to a bid showing the quantity of energy that an agent (in this case the building) is willing to consume at a given price [Hao 16]. Demand curves can be plotted by performing the multi period optimization for different prices profiles. An arbitrary starting point is chosen as 12:00 pm for one of the test days with all the zone temperatures at 22.5 $^{O}$C. A constant price at 0.4 p.u. is considered for a three steps ahead prediction (*i.e.* 15 min). The value attached to the first time step is then progressively changed in the range [0,1] and the GAMS optimization is launched for every new price profile. The simulation is performed for different building settings.

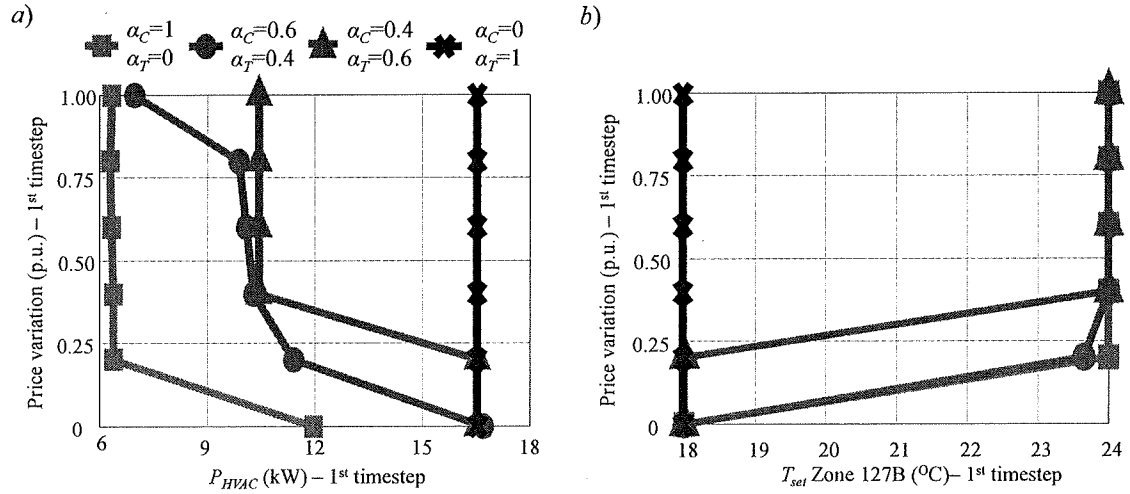


Fig.18 Cost Minimization Vs Comfort - *a)* Demand Curve - *b)* Associated set-points

Fig.18*a* shows the demand curve for different arbitrages between cost savings and comfort, keeping $\alpha_E = 0$ in all cases. Only $P_{hvac}$ for the first time step is considered here. The blue line (square markers) corresponds to the case where maximum priority is given to cost minimization. The HVAC power then has a low value. The energy consumed during the first period remains constant no matter the price except when it is at its lower bound (0 p.u.) where an increment is noticed – meaning that the building is willing to absorb more power for extremely low prices. Moving the priority progressively towards more comfort priority, the demand curve shifts progressively towards another extreme (black curve with cross markers), where, no matter the price, the energy consumed remains constant to achieve the temperature for maximum comfort (*i.e.* dropping from 22.5 $^{O}$C to 21.0 $^{O}$C). Fig.18*b* shows the corresponding temperature settings for Zone 1 ("corridor"). Depending on the priority given to cost or comfort, this temperature setting is either minimum (18°C) or maximum (22.5 $^{O}$C) except for very low prices.

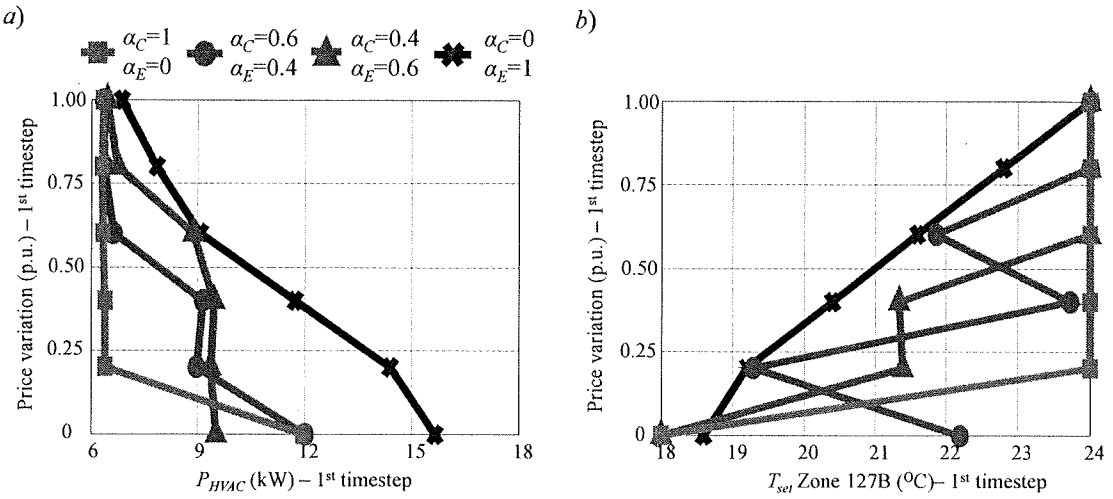


Fig.19 Cost Minimization Vs Elasticity - *a)* Demand Curve - *b)* Associated set-points

If a weight of zero is given to the flexibility component of the objective (i.e. $\alpha_E = 0$), the power consumption of the building exhibits an insignificant price elasticity. As shown in Fig.18*b*, the temperature set points are set at one limit or the other irrespective of the price. This underlines the fact that in a transactive framework another objective has to be added in order to represent the willingness of the building to respond to outside incentives. Fig.19*a* shows the demand curves obtained after the introduction of the price elasticity objective in the utility function and moving from minimum cost priority to maximum flexibility ($\alpha_T = 0$ in all cases). The blue curve (square markers) is the same as in Fig.18*a* with the cost priority. As the weight given to flexibility increases, $P_{hvac}$ acquires a smoother dependence on the price. Fig.19*b* shows that the set points do not move from one bound to another.

# 4 SUPPLIER-BUILDING INTERACTIONS

## 4.1 Bi-level Optimization

### 4.1.1 Formulation

As mentioned before, the objective of this project is to incorporate HVAC control in the multi-step transactive framework as illustrated in Fig.1*b*. At each iteration, the MPC for every device returns the predicted power demand profile corresponding to a particular price profile based on the buildings model and settings (comfort, cost saving, *etc.*). The optimal solution is determined by the supplier side objective (balance demand-supply, regulation, *etc.*). Once the optimal TS profile has been found, it is sent to the devices in order to schedule their controls for the upcoming time periods.

In this study the supplier side objective is assumed to be to follow a predefined mean power profile $P_{target}$ for each hour $h$. This profile corresponds to the profile of energy purchased by the supplier. In order to limit the computational time, the method to find the appropriate TS relies on a bi-level optimization (Fig.20). Interpreting a multi period demand curve in a multi-step framework is not trivial and evaluating all the prices combination over time could lead to a CPU time greater than the time step itself.

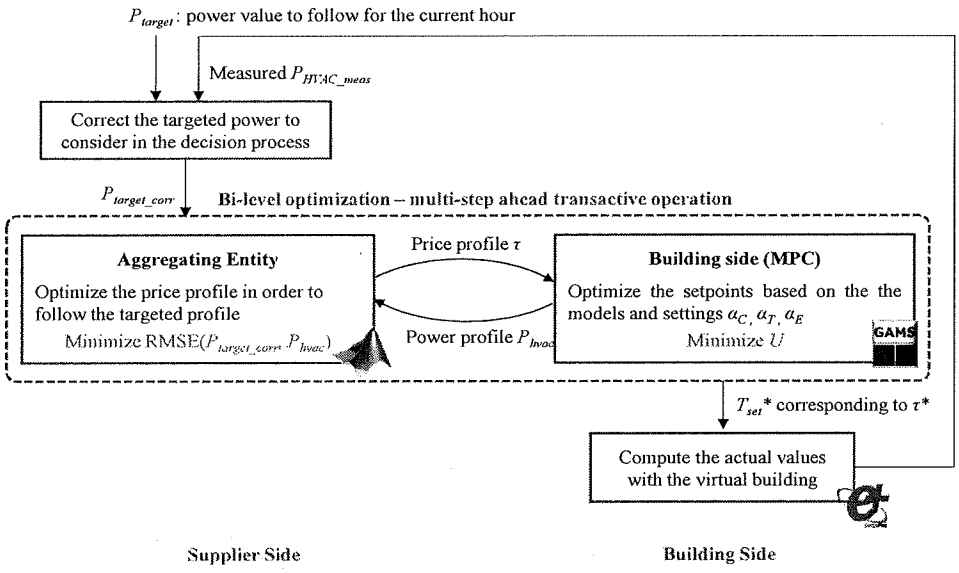


Fig.20: Bi-level optimization for multi steps ahead transaction

The bi-level optimization is performed on a rolling basis with a multi step decision making process from $T_{start}$ to $T_{end}$. The objective is to find the optimal price profile $\boldsymbol{\tau}^*$ that correspond to a consumed $P_{hvac}$ profile that allows following the targeted power for the corresponding hour. As the control of the building is based on MPC, the measured power $P_{hvac\_meas}$ (calculated using the Energy+ model) is different from the forecast value. Thus the power to follow is corrected intra hour to obtain $P_{target\_corr}$ using Eq.17 in order to mitigate the deviations observed for the previous time steps. The aggregating entity objective function is then expressed as the RMSE between the $P_{hvac}$ profile returned by the MPC controller and the corrected targeted power (Eq.18). Note that the TS are considered as price-like signal with no specified scale. Thus normalized values between 0 p.u. and 1 p.u. are used in the implementation.

$$P_{target} = \frac{1}{1\text{h}}\left(\sum_{t=h}^{t=T_{start}} P_{hvac\_meas}(t) + (h+1-T_{start}) \times P_{target\_corr}\right) \qquad \textbf{Eq.17}$$

$$\boldsymbol{\tau}^* = \underset{0p.u.\le\tau\le1p.u.}{\arg\min}\left(\sqrt{\frac{1}{T_{end}-T_{start}}\sum_{t=T_{start}}^{t=T_{end}}\left(P_{target\_corr}-P_{hvac}(t)\right)^2}\right) \qquad \textbf{Eq.18}$$

On the building side, the MPC calculates the output $P_{hvac}$ profile corresponding to the received TS profile. The building response depends on its settings, i.e. on the relative weight given to cost minimization, comfort or elasticity. Obviously the ability of the aggregating entity to follow its own objective is strongly affected by the building preferences.

### 4.1.2 Search Algorithms

Two search algorithms are tested for optimizing the price profile in the multi step transaction framework: a Particle Swarm Optimization (PSO) and a Greedy Algorithm (GD). Fig.21*a* shows the flow diagram for the Particle Swarm Optimization algorithm. Fig.21*b* illustrates how the position of the swarm of particles evolves in the search space. This movement involves three components:

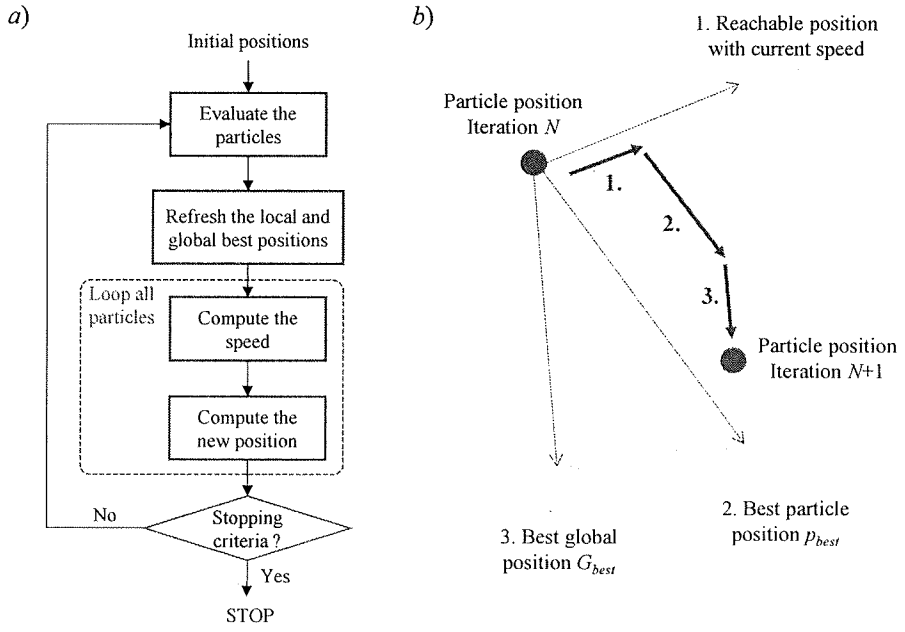


Fig.21: PSO – *a)* architecture – *b)* refreshment of particles positions

- **A physical component:** every particle tends to pursue its movement depending on an inertia facto $\omega$
- **A cognitive component:** every particle tends to be attracted by its best known position ($p_{best}$) observed during past iterations
- **A social component:** every particle tends to be attracted by the best known position for the whole swarm ($G_{best}$)

Two acceleration coefficients $c_1$ and $c_2$ are associated with the cognitive and social components. At each iteration the speed (and therefore the position) of every particle is computed according to Eq.19 with $r_1$ and $r_2$ two random coefficients sample using a uniform distribution [Kennedy 95]. $i$ represents the $i^{th}$ parameter of particle $p$. In this application, each particle is a profile, the parameters are the prices from $T_{start}$ to $T_{end}$ and the particle evaluation correspond to the GAMS optimization using the MPC implementation. The stopping criteria involve the maximum number of iterations, the computing time and non-improvement conditions. The values of $\omega$, $c_1$ and $c_2$ as well as the number of particles have a direct impact on the performance of the method, because they define the balance the exploration of the search space and intensification of the search around interesting solutions. Based on [Trelea 03], these parameters were selected as follows: $\omega = 0.72$, $c_1 = c_2 = 1.49$.

$$V_i(N) = \omega \times V_i(N-1) + c_1 \times r_1 \times (p_i - p_{best}) + c_2 \times r_2 \times (p_i - G_{best}) \qquad \textbf{Eq.19}$$

Fig.22 shows the architecture of a traditional greedy algorithm (GD). From a given starting point, the method progressively explores the nD neighborhood with a specified discretization of the search space. Two options of full factorial design are possible to perform the exploration. At each iteration the best solution is saved as the central point of the next step. The procedure stops when no improvement is performed, when the bounds of the search space are reached or when a maximum number of evaluations has been processed. Then the algorithm is launched again with a finer discretization using the previous

best solution as a new starting point. The algorithm stops when a minimum discretization has been achieved.

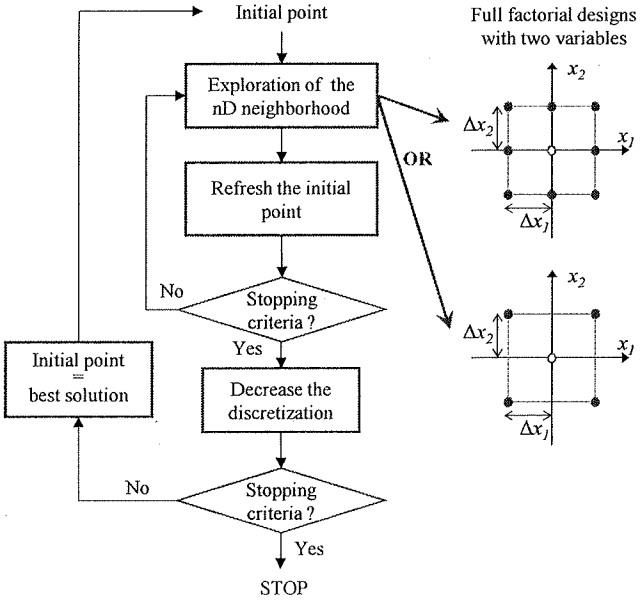


Fig.22: Greedy algorithm

## 4.2 Test Results

### 4.2.1 Case study

The proposed approach is first tested with a single building (the SEB building) for August 20th and the Typical Meteorological Year (TMY) data. The baseline corresponds to a case where all the set points are constant at 22.5 °C all day long. To limit the simulation time and put the emphasis on the impact of the MPC strategy as compared to the baseline case, the interactions between the building and the supplier are tested from 1200 to 1500 h with the flowing arbitrary chosen values:

- From 12:00 to 13:00 – $P_{target}$ = 12 kW
- From 12:00 to 13:00 – $P_{target}$ = 7 kW
- From 12:00 to 13:00 – $P_{target}$ = 9.5 kW

The PSO algorithm uses 10 particles and a maximum number of 20 iterations with the initial position determined using Latin Hypercubes in order to get a random sampling that is uniformly distributed in the search space [Mckay 00].The greedy algorithm is launched using the last recorded price as the initial point along the optimization horizon (initial value at 0.5 p.u.). The search space (price profile) discretization is progressively decreased for 0.2 p.u. to 0.025 p.u.

### 4.2.2 Priority to elasticity

At first the transactive framework is tested with the SEB building giving priority to elasticity ($\alpha_E = 1$, $\alpha_C = \alpha_T = 0$), *i.e.* a strong willingness to respond to incentives. A first simulation is performed using the greedy method. Fig.23*a* shows the resulting HVAC power profile compared to the baseline case

with higher value from 1200 to 1300 and a decrease observed from 1300 to 1400 h as expected. On Fig.23*b* the actual profile of the virtual building displays strong oscillations that were not predicted and the mean energy diverge from the targeted value of 9.5 kWh. The zone temperature Fig.23*c* as well as the final TS profile Fig.23*d* are consistent with lower values when a higher power is desired and lower values when it tries to reduce energy consumption.

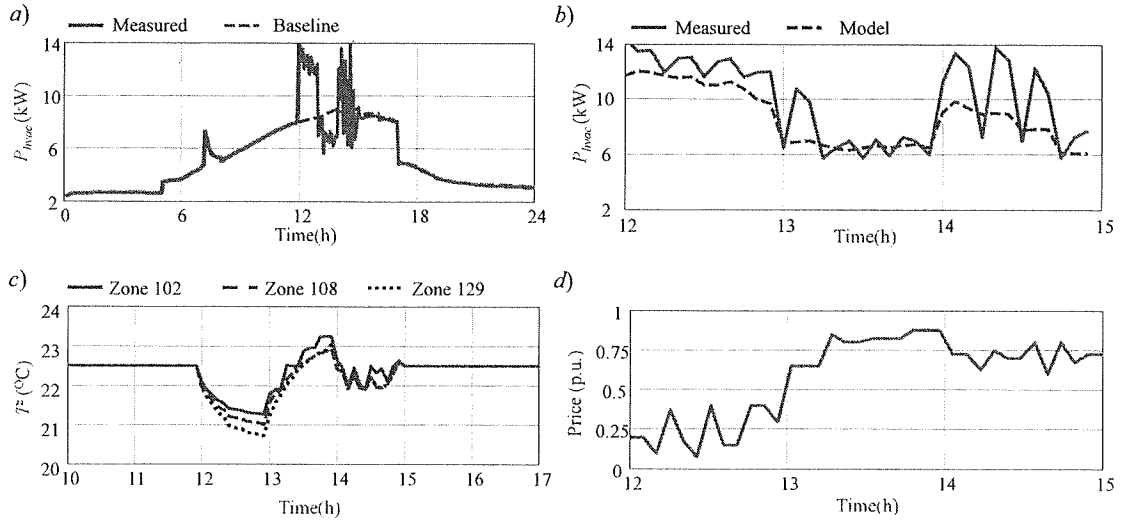


Fig.23: Preliminary results - *a)* $P_{hvac}$ - *b)* $P_{hvac}$ prediction - *c)* Zone temperatures - *d)* Price profile

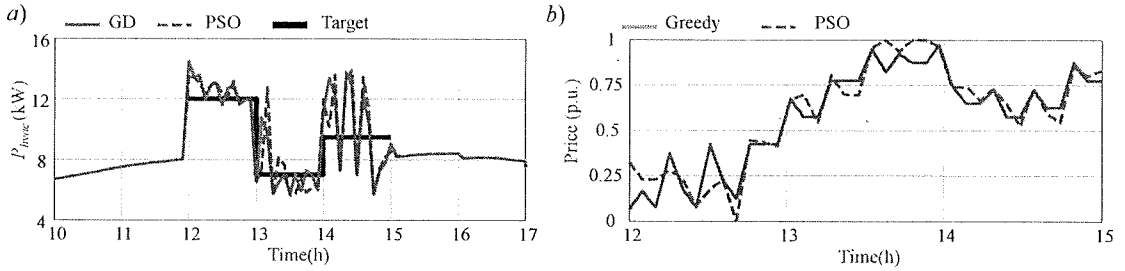


Fig.24: Greedy Method Vs PSO algorithm - *a)* HVAC power - *b)* Price profile

Fig.24 and Table 1 compares the results obtained with the greedy method and with the PSO for the same case study with priority given to elasticity. The results obtained with these two methods are very close and produce similar error compared to the target values are observed from 1200 to 1500 h. However, the greedy method is less time consuming than the PSO. On average the bi-level optimization performed every 15 min requires 55 calls of the objective function (*i.e.* MPC optimization here) while the PSO performs 106 runs. As with the greedy method, the results obtained with the PSO from 1400 to 1500 h show strong HVAC power oscillations and a significant deviation from the target value set of 9.5 kWh. This stems from a behavior of the virtual building that is not well predicted by the model and results in high RMSE and relative error values between the forecast and the measures (Table 1).

Table 1: Obtained Results for priority given to elasticity

| | Energy Consumed from 12:00 to 13:00 | Energy Consumed from 13:00 to 14:00 | Energy Consumed from 14:00 to 15:00 | RMSE $P_{hvac}$ | Relative Error $P_{hvac}$ |
|---|---|---|---|---|---|
| **Target** | 12 kWh | 7 kWh | 9.5 kWh | - | - |
| **GD** | 12.7 kWh (error: 6 %) | 6.9 kWh (error: 1 %) | 10.4 kWh (error: 10 %) | 2.1 kWh | 14 % |
| **PSO** | 12.6 kWh (error: 5 %) | 7.0 kWh (error: 0 %) | 10.2 kWh (error: 7 %) | 2.2 kW | 15 % |

In an attempt to reduce these oscillations and the error, a term was added in the objective function of the aggregating entity in order to smooth the prices and consequently the set point profile. As expressed in Eq.20 the goal is to ensure that the product $(\tau(t)-\tau(t-1))\times(\tau(t+1)-\tau(t))$ is positive. Then $C_{osc}$ is null whenever the constraint is fulfilled and positive otherwise. To ensure the convergence of the search method the constraint is included in the RMSE minimization in Eq.21 with a penalty factor $\lambda$ (typically $10^6$).

$$C_{osc}(t) = -\min\left(\left(\tau(t)-\tau(t-1)\right)\times\left(\tau(t+1)-\tau(t)\right),0\right) \quad \textbf{Eq.20}$$

$$\boldsymbol{\tau}^* = \underset{0\,p.u.\le\tau\le 1\,p.u.}{\arg\min}\left(\sqrt{\frac{1}{T_{end}-T_{start}}\sum_{t=T_{start}}^{t=T_{end}}\left(P_{target\_corr}-P_{hvac}(t)\right)^2+\lambda\times C_{osc}(t)}\right) \quad \textbf{Eq.21}$$

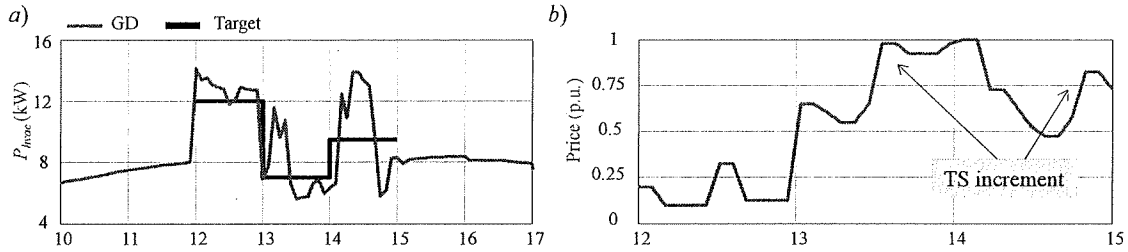


Fig.25: Greedy Method and price oscillation constraint- *a)* HVAC power - *b)* Price profile

Fig.24 shows the results obtained under the same conditions with the greedy method and the updated objective function on the aggregating entity side. As expected the resulting price profile is smoother. It is worth noticing that before 14:00 and 15:00 the TS signal tends to increase in order to lower the energy consumed to match the hourly target values. For the first period after 13:00 (the same for 14:00) the observed power is higher than the target value. Therefore, in order to reach the desired hourly energy, $P_{target}$ is lowered by increasing the price signal. Table 2 shows the final values for hourly energy with an error of 7% compared to the target value, and with a lower RMSE than previously for the HVAC power prediction.

Table 2: Obtained Results with the oscillation constraint added

| | Consumed energy from 1200 to 1300 h | Consumed energy from 1200 to 1300 h | Consumed energy from 1200 to 1300 h | RMSE $P_{hvac}$ | Relative Error $P_{hvac}$ |
|---|---|---|---|---|---|
| **Greedy ($C_{osc}$)** | 12.8 kWh (error: 6 %) | 7.1 kWh (error: 1 %) | 10.0 kWh (error: 5 %) | 1.7 kW | 12 % |

### 4.2.3 Other priorities

Another test is performed with the priority given to the cost minimization ($\alpha_C = 1$, $\alpha_T = \alpha_E = 0$) with the same target power/energy profile. For those settings the building is supposed to be non-responsive to any incentive as it will try to lower the consumed energy as much as possible. A preliminary test led to the results shown on Fig.26*a*. While the energy consumed tends to be lower, strong oscillations can be observed and the resulting zone temperatures do not necessary increase to minimize energy consumption in cooling mode. In that case a new constraint is introduced to maintain the set points at a constant value for the prediction horizon from $T_{start}$ to $T_{end}$. Fig.27 shows that this results in lower energy consumption from 1200 to 1500 h. The zone temperatures tends to increase, especially in zone 129 where the upper bound is reached.

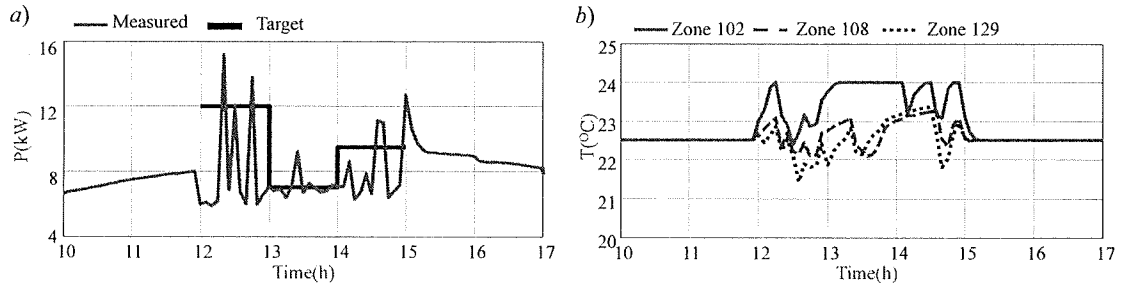


Fig.26: Cost priority without set points constraint - *a)* HVAC power - *b)* Zone temperature

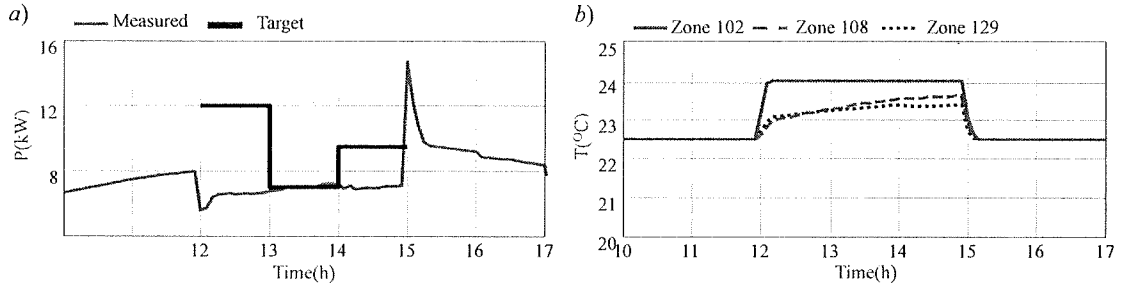


Fig.27: Cost priority with set points constraint - *a)* HVAC power - *b)* Zone temperature

A case with priority given to comfort was also investigated ($\alpha_T = 1$, $\alpha_c = \alpha_E = 0$), *i.e.* a building that does not respond to incentives and has constant set points over the optimization horizon. Fig.28 shows that all the observed zone temperatures tend to reach the reference value set of 21 °C while the energy consumed remains high. There is no point in interpreting the price profile resulting from the bi-level optimization for these building settings. For instance, running the GD algorithm the search method would detect a non-improvement of the solution by exploring the search space around the initial point. The resulting price profile would be flat and equal to the arbitrary initial point value of 0.5 p.u..

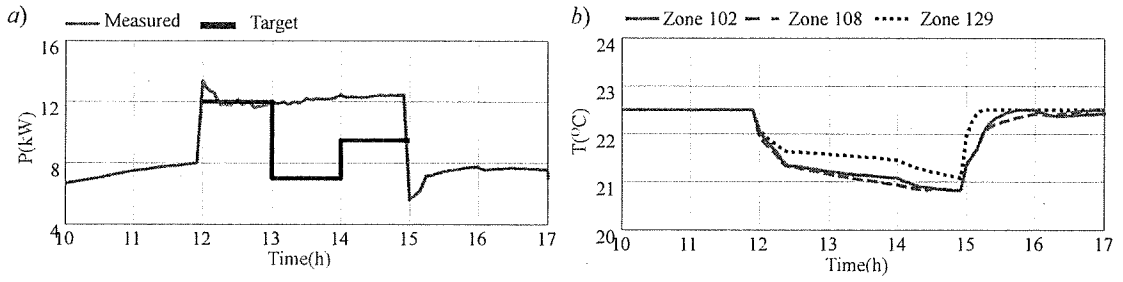

Fig.28: Results with comfort priority - *a)* HVAC power- *b)* Zone temperatures

# 5 MANAGING MULTIPLE BUILDINGS

## 5.1 Thermal load model

The previous section considered only one building. We now consider the case where multiple buildings are managed in a transactive framework. In a central optimization approach managing a large number of buildings requires too much computing resources. Reduced order model [Iacovella 16] or model free [Ruelens 14Ruelens 14] approaches achieve acceptable computing times for up to 1000 loads. As already mentioned, one of the advantages of the transactive control is its scalability with a distributed intelligence using an agent-based approach as in [Zhou 11]. Thus each building is independently managed depending on its own setting and following the strategy described in section 3.2.

In this section, we consider fictitious buildings. They are represented as a single zone with simple thermostatically controlled loads (TCL) whose behavior is predicted by equation Eq.22 [Hao 15] and the discrete formulation shown Eq.23. $T$ and $T_{out}$ represent respectively the indoor and outdoor temperatures. $R_{th}$ and $C_{th}$ are the thermal resistance and capacitance of the building while $COP$ is the coefficient of performance attached to the HVAC system. As previously $P_{hvac}$ is the HVAC power (associated with the cooling or heating energy).

$$\frac{dT}{dt} = -a \times (T - T_{out}) - b \times P_{hvac} \quad \text{with} \quad a = \frac{1}{R_{th} \times C_{th}} \quad \text{and} \quad b = \frac{COP}{C_{th}} \qquad \textbf{Eq.22}$$

$$T(t+1) = T(t) - a \times (T(t) - T_{out}(t)) \times dt - b \times P_{hvac}(t) \times dt \qquad \textbf{Eq.23}$$

In the stationary state, the power required to keep the indoor temperature at a desired set point $T_s$ is given by Eq.24. The assumption is made that every time the set point is changed, the resulting HVAC power is equal to the $P_{hvac}$ required to maintain T at the desired value.

$$P_{hvac}(t) = \frac{T_{out}(t) - T_{set}(t)}{R_{th} \times COP} \qquad \textbf{Eq.24}$$

In this case study, the building is in cooling mode with $T_{set}$ between $T_{set\_min} = 18°C$ and $T_{s\_max} = 24°C$. A maximum expected value for the HVAC power $P_{hvac\_max}$ is then computed considering the minimum setpoints with the highest expected outdoor temperature $T_{out\_max}$ arbitrarily set at 45 °C here (Eq.25).

$$P_{hvac\_max} = \frac{T_{out\_max} - T_{set\_min}}{R_{th} \times COP} \qquad \textbf{Eq.25}$$

Depending on the time step (*e.g.* early in the morning) the outdoor temperature could possibly be lower than the specified set point. In that case the HVAC system would heat the building resulting in a negative value for $P_{hvac}$. For these time steps, we make the strong hypothesis that the electrical behavior of the system is symmetrical in cooling or heating mode by assuming $P_{hvac}(t) = |P(t)|$. This is somewhat unrealistic. The outdoor temperature profile used in the previous section is considered for these simulations as well. Different TCLs are then generated with $R_{th}$ and $C_{th}$ values with a uniform distribution $U_n$ (Table 3).

Table 3: TCL models parameters

| Parameter | Description | Value | Unit |
|---|---|---|---|
| $R_{th}$ | thermal resistance | 2 + $U_n$(0, 0.5) | $^{O}$C/kW |
| $C_{th}$ | thermal capacitance | 2 + $U_n$(0, 0.5) | kWh/$^{O}$C |
| $COP$ | coefficient of performance | 3 + $U_n$(0, 3) | - |
| $T_{out\_max}$ | design outdoor temperature | 40 | $^{O}$C |
| $T_{set\_min}$ | minimum design setpoint | 18 | $^{O}$C |

## 5.2 Implementation

Simulations are run using the implementation illustrated in Fig.29. Here the transactive operation considers multiple buildings represented with simple TCL models. In the bi-level optimization process the transactive signal TS is sent simultaneously to the model of each building, which returns its response. On the supplier, side the decision making process then consider the cumulated load in order to choose the most appropriate price profile.

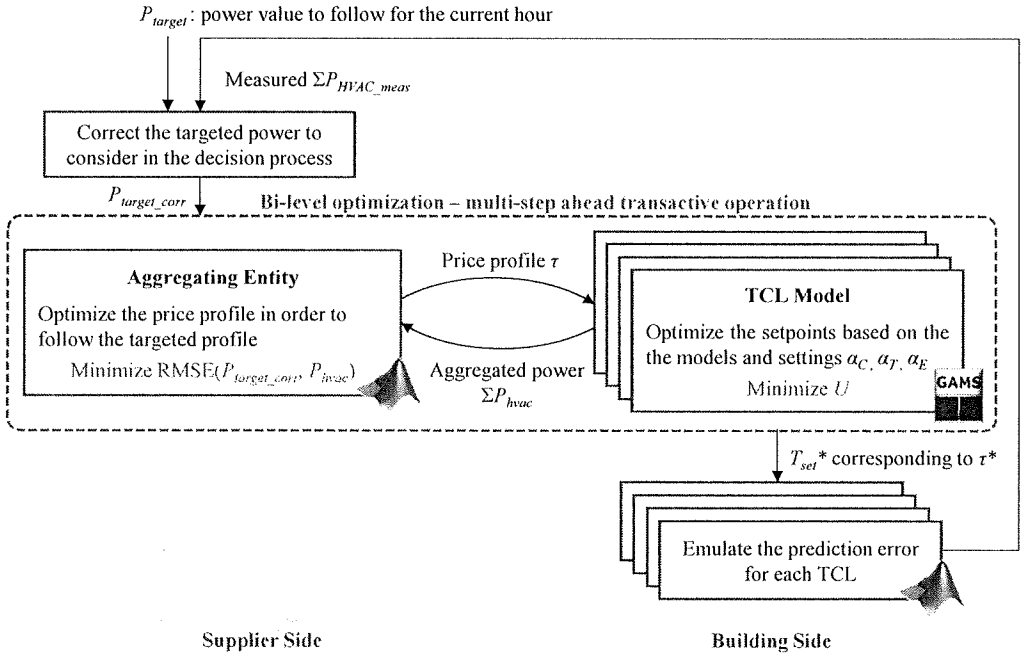


Fig.29: Transactive operation with multiple fictitious TCL

As seen in the previous section the prediction error in a MPC framework can lead to strong deviations from the optimized power values. That is why a correction method has been added to adapt the targeted power. When considering the SEB, the building simulation using the Energy+ model made it possible to compute the forecast error. With the simple TCL model the prediction uncertainties for $P_{hvac}$ are modeled using a normal distribution $N_0$ and a mean relative error shown on Fig.16*a* ; 5 % for one step ahead, 7.5 % for two steps ahead, 10 % for three steps ahead, *etc.*. When the MPC is processed, a fictitious measured $P_{hvac\_meas}$ is computed starting from the predicted optimal $P^*_{hvac}$ returned by the model for every building. Here $t$ refers to the prediction horizon with the numbers of steps ahead that are considered. Applying Eq.26, an emulated error is then generated ensuring a monotone increase in uncertainty over time using both the max and sign functions.

$$\begin{cases} \text{if } t = 1 \text{ then } \varepsilon(t) = \mathrm{N}_o(0,0.05) \\ \text{else } \varepsilon(t) = \max\left(\left|\varepsilon(t-1)\right|, \left|\mathrm{N}_o(0,0.05+0.025\times(t-1))\right|\right)\times \text{sign}\left(P_{hvac\_meas}(t-1) - P^*_{hvac}(t-1)\right) \\ P_{hvac\_meas}(t) = \left(1+\varepsilon(t)\right)\times P^*_{hvac}(t) \end{cases} \quad \textbf{Eq.26}$$

## 5.3 Results

Ten heterogeneous TCL were generated using the parameters given in Table 3. Once again to limit the computational time and highlight the effects of the MPC, the transactive simulation is limited to the period from 12:00 to 15:00. The targeted hourly mean power to follow is arbitrarily defined and is expressed as a function of the aggregated maximum HVAC power for all the buildings:

- From 1200 to 1300 h – $P_{target} = 0.6\times\Sigma P_{hvac\_max}$
- From 1200 to 1300 h – $P_{target} = 0.4\times\Sigma P_{hvac\_max}$
- From 1200 to 1300 h – $P_{target} = 0.8\times\Sigma P_{hvac\_max}$

Three different scenarios are investigated by varying the buildings settings and moving from a priority given to elasticity ($\alpha_E = 1$ for all loads) to priority given to comfort ($\alpha_T = 1$ for all loads). As in the previous simulations the greedy method is used to find the TS. The results displayed on Fig.30*a* show that the overall ability to respond to incentives obviously decreases when more buildings become "uncontrollable" in order to fulfil the comfort requirement. From 1300 to 1400 h the targeted profile cannot be reached even with 100 % of the TCL set to a maximum flexibility. This level of power consumption is unreachable given the outdoor temperature and the characteristics of the buildings. Fig.30*b* shows the evolution of the mean temperature computed considering all the loads. As expected strong deviations around the reference value (21 $^{O}$C) are observed when priority is given to flexibility. These deviations allows following the targeted power with lower temperature changes for a given consumption profile. When the proportion of building that favor comfort increases, the magnitude of the observed oscillations decreases to reach a case where the average temperature is equal to the reference values for all the building with $\alpha_T = 1$.

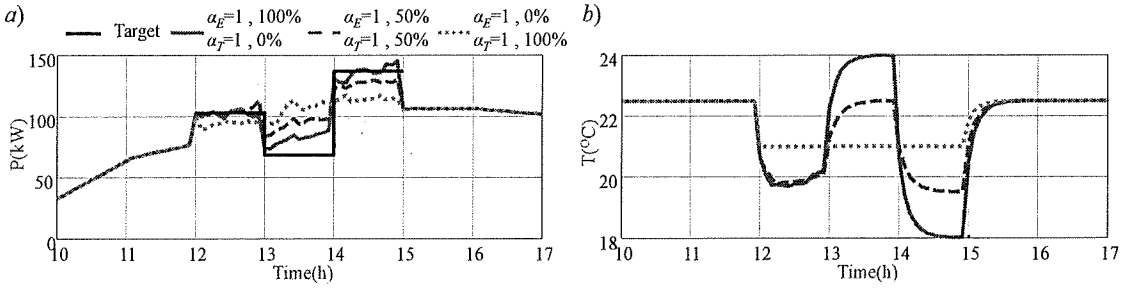


Fig.30: Results for multi TCL simulation – *a)* aggregated HVAC power – *b)* mean temperature

An additional set of simulations was run by varying the number of buildings in order to estimate the final observed prediction error of the aggregated load. The RMSE (normalized using $\Sigma P_{hvac\_max}$) and the mean relative error were computed by comparing the overall power profile computed by the MPC with the values generated using Eq.26. As expected, with wide spread heterogeneous loads, the results show a monotonic decrease when the number of TCL increases (Fig.31). Managing a larger number of loads then mitigates the forecast errors resulting from the use of model predictive control for the buildings considered.

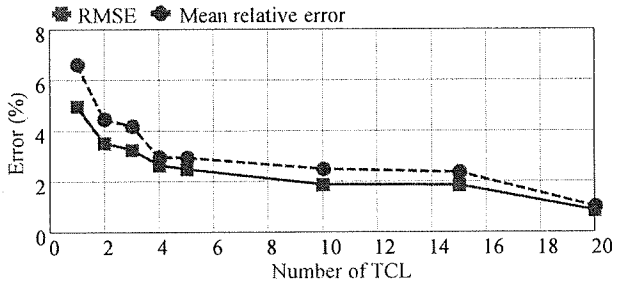


Fig.31: Error Vs number of simulated TCL

# CONCLUSIONS

This report describes the implementation of a HVAC system management with MPC in a multi-step transactive framework. This framework implements a bi-level optimization and ensures that an objective on the supplier side (*i.e.* follow a predefined power profile) can be achieved. In particular, the results highlight the fact that the success of the procedure is closely linked to the preferences of the set of buildings under control. If al buildings require maximum comfort, no flexibility can be obtained. Adding an "elasticity" components to the objective function enhances the flexibility provided by the building compared to the conventional approach that performs a tradeoff between energy savings and comfort.

Further work should investigate the following topics:

- Neural Network were shown to be appropriate for multi-period forecasts. However significant deviations from the model were observed when simulating the control loop. The performance of the model should therefore be improved by improving the training data set to match better the conditions under which the HVAC will be used with the implemented MPC. A constrained fitting of the weights and bias could also be introduced to ensure the fulfillment of the physical constraints.

- In the simulations, the objective of the supplier was to follow an arbitrary defined power profile. Further studies should investigate different ways of generating this input. For instance, a day-ahead unit commitment with the building models as storage devices added to inelastic load could be used to create such a profile.

- Finally, while the first surveys using the transactive approach mostly referred to conventional building loads, the method could be extended easily to other types of devices (e.g. electrical vehicles in [Behboodi 16]) as long as a bidding curves can be developed. Future studies should then consider systems with heterogeneous devices, including controllable and uncontrollable loads, renewable energy sources and storage units with different utility functions and responses depending on the transactive signals.

# REFERENCES


Behboodi 16 — S. Behboodi, D. Chassin, C. Crawford, N. Djilali, "Electric Vehicle Participation in Transactive Power Systems Using Real-time Retail Prices", 49th Hawaii International Conference on System Sciences, Koloa, United-States, pp. 2400–2407, 2016

Bernal 12 — W. Bernal, M. Behl, T.X. Nghiem, R. Mangharam, "MLE+: A Tool for Integrated Design and Deployment of Energy Efficient Building Controls", Buildsys'12, Toronto, ON, Canada, 2012

Boné 02 — R. Boné, M. Crucianu, "Multi-step-ahead prediction with neural networks: a review. Publication", 9èmes rencontres internationales « Approches Connexionnistes en Sciences Économiques et en Gestion », Boulogne sur Mer, France. 2002

EIA 16 — US Energy Information Administration - Commercial Buildings Energy Consumption Survey (2012), https://www.eia.gov/consumption/commercial/reports/2012/energyusage/ Results released in 2016

Fanger 72 — P.O. Fanger, "Thermal Comfort: Analysis and Applications in Environmental Engineering", McGraw-Hill, New York, 1972.

Fereira 12 — P.M. Ferreira, A.E. Ruano, S. Silva , E.Z.E. Conceicao, "Neural networks based predictive control for thermal comfort and energy savings in public buildings", Energy and Buildings, Vol. 55, pp. 989–993, 2012

Foucquier 13 — M. Foucquier, S. Robert, F. Suarda, L. Stéphan, A. Jay, "Annual electricity consumption forecasting by neural network in high energy consuming industrial sectors", Energy Conversion and Management, Vol. 49, pp. 2272–2278, 2013

Gossard 13 — D. Gossard, B. Lartigue, F. Thellier ; "Multi-objective optimization of a building envelope for thermal performance using genetic algorithms and artificial neural network", Energy and Buildings, Vol. 63, pp. 253–260, 2013

Hagan 94 — M.T. Hagan, M. Menhaj, "Training feed-forward networks with the Marquardt algorithm", IEEE Transactions on Neural Networks, Vol. 5, No. 6, 1999, pp. 989–993, 1994.

Hammerstrom 07 — D.J. Hammerstrom and all, "Pacific Northwest GridWise™ Testbed Demonstration Projects , Part I. Olympic Peninsula Project", Report Pacific Northwest National Laboratory, 2007

Hao 15 — H. Hao, B.M. Sanandaji, K. Poolla, T.L. Vincent, "Aggregate Flexibility of Thermostatically Controlled Loads", IEEE Transactions on Power Systems, Vol. 30, pp. 189–198, 2015

Hao 16 — H Hao, C.D. Corbin, K. Kalsi, R.G. Pratt, "Transactive Control of Commercial Buildings for Demand Response", IEEE Transactions on Power Systems, 2016

Iacovella 16 — S. Iacovella, F. Ruelens, P. Vingerhoets, B. Claessens, G. Deconinck, "Cluster Control of Heterogeneous Thermostatically Controlled Loads Using Tracer Devices", IEEE Transactions on Smart Grid, 2016

Kennedy 95 — J. Kennedy, R. Eberhart, "Particle swarm optimization", Proceedings of the IEEE international conference on neural networks,1995

Kok 16 — K. Kok, S. Widergren, "A Society of Devices: Integrating Intelligent Distributed Resources with Transactive Energy", IEEE Power and Energy Magazine, Vol. 14, 2016

Kusiak 14 R. Kusiak, G. Xu, Z. Zhang, "Minimization of energy consumption in HVAC systems with data-driven models and an interior-point method", Energy Conversion and Management, Vol. 85, pp. 146–153, 2014

Lee 15 Y.M. Lee, R. Horesh, L. Liberty, "Simulaton and optimzation of energy efficient operation of HVAC system as demand response with distributed energy resources", Winter Simulation Conference, Huntington Beach, CA, United-States, 2015

Ma 11 J. Ma, S.J. Qin, B. Li, T. Salsbury, "Economic model predictive control for building energy systems", Innovative Smart Grid Technologies (ISGT) Conference, Hilton Anaheim, CA, United-States, 2011

Macas 16 M. Macas, F. Moretti, A. Fonti, A. Giantomassi, G. Comodic, M. Annunziatob, S. Pizzuti, A. Capra, "The role of data sample size and dimensionality in neural network based forecasting of building heating related variables", Energy and Buildings, Vol. 111, pp. 299–310, 2016

Magnier 10 L. Magnier, F. Haghighat, "Multiobjective optimization of building design using TRNSYS simulations, genetic algorithm, and Artificial Neural Network", Building and Environment, Vol. 45, 739–746, 2010

Mckay 00 M.D. Mckay, R. J. Beckman, W.J. Conover, "A Comparison of Three Methods for Selecting Values of Input Variables in the Analysis of Output From a Computer Code", Technometrics, 42:1, pp. 55-61, 2000

Patteeuw 15 D. Patteeuw, K. Bruninx, A. Arteconi, E. Delarue, W. D'haeseleer, L. Helsen, "Integrated modeling of active demand response with electric heating systems coupled to thermal energy storage systems", Applied Energy, Vol. 151, pp. 989–993, 2015

Plaudel 14 S. Paudel, M. Elmtirib, W.L. Kling, O. Le Correa, B. Lacarrière, "Pseudo dynamic transitional modeling of building heating energy demand using artificial neural network", Energy and Buildings, Vol. 56, pp. 81–93, 2014

Privara 13 S. Prívaraa, J. Cigler, Z. Vánaa, F. Oldewurtelb, C. Sagerschnigc, E. Zácekováa, "Building modeling as a crucial part for building predictive control", Energy and Buildings, Vol. 56, pp. 8–22, 2013

Raza 15 M. Qamar, A. Khosravi, "A review on artificial intelligence based load demand forecasting Techniques for smart grid and buildings", Renewable and Sustainable Energy Reviews, Vol. 50, pp. 1352–1372, 2015

Ruelens 14 F. Ruelens, B. J. Claessens, S. Vandael, S. Iacovella, P. Vingerhoets, R. Belmans, "Demand Response of a Heterogeneous Cluster of Electric Water Heaters Using Batch Reinforcement Learning", IEEE Power Systems Computation Conference (PSCC), Wroclaw, Poland, 2014

Schneider 11 K.P. Schneider, J.C. Fuller, D. Chassin, "Analysis of Distribution Level Residential Demand Response", Power Systems Conference and Exposition, Phoenix, United-States, 2011

Subbarao 13 K. Subbarao, J. Fuller, K. Kalsi, R. Pratt, S. Widergren, D Chassin,"Transactive control and coordination of distributed assets for ancillary services". Richland, WA: Pacific Northwest National Lab ; 2013

Trelea 03 I.C. Trelea, "The particle swarm optimization algorithm: convergence analysis and parameter selection", Information Processing Letters, Vol. 85, pp. 317–325, 2003

| | |
|---|---|
| Yu 11 | H. Yu, B.M. Wilamowski, "Levenberg–Marquardt training", The Industrial Electronics Handbook, Intelligent Systems, vol. 5, second ed., CRC Press, Boca Raton, 2011 |
| Yuce 14 | B. Yuce, H. Li, Y. Rezgui, I. Petri, B. Jayan, C. Yang, "Utilizing artificial neural network to predict energy consumption and thermal comfort level: An indoor swimming pool case studyBaris", Energy and Buildings, Vol. 80, pp. 45–56, 2014 |
| Zaheer 04 | M. Zaheer-Uddin, N. Tudoroiu, "Neuro-models for discharge air temperature system", Energy Conversion and Management, Vol. 45, pp. 901–910, 2004 |
| Zhao 13 | J. Zhao, K.P. Lam, B.E. Ydstie, "EnergyPlus Model-Based Predictive Control (EPMPC) by Using Matlab/Simulink and MLE+", 13th Conference of International Building Performance Simulation Association, Chambéry, France, 2013 |
| Zhou 11 | Z. Zhou, F. Zhao, J. Wang, "Agent-Based Electricity Market Simulation With Demand Response From Commercial Buildings", IEEE Transactions on Smart Grid, Vol. 2, pp. 580–588, 2011 |

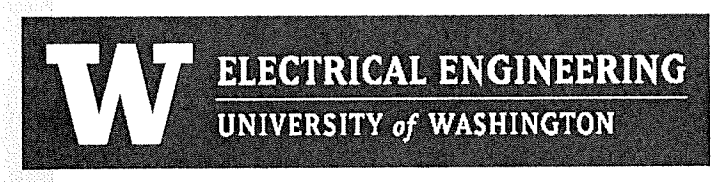


University of Washington
Department of Electrical Engineering
185 Stevens Way
Paul Allen Center - Room AE100R
Campus Box 352500
Seattle, WA 98195-2500